

The influence of iron substitution on the magnetic properties of hausmannite, $\text{Mn}^{2+}(\text{Fe},\text{Mn})_2^{3+}\text{O}_4$

V. BARON,^{1,*} J. GUTZMER,² H. RUNDLÖF,³ AND R. TELLGREN³

¹The Studsvik Neutron Research Laboratory, S-611 82 Nyköping, Sweden

²Department of Geology, Rand Afrikaans University, P.O. Box 524, Auckland Park 2006, Johannesburg, South Africa

³Inorganic Chemistry, Ångström Laboratory, Uppsala University, Box 538, S-751 21 Uppsala, Sweden

ABSTRACT

The occurrence of hausmannite with an apparent Curie temperature close to 750 K, instead of 41.8 K was recently described from hydrothermally altered manganese ore from the Kalahari manganese field, South Africa. The unusual magnetic properties were related to the substitution of Fe^{3+} for Mn in the hausmannite structure. Because of the large differences in the scattering lengths of Fe and Mn, $b_{\text{Fe}} = 9.94$ and $b_{\text{Mn}} = -3.73$ fm, respectively, we performed neutron powder diffraction experiments at 295 and 10 K on natural mineral separates and synthetic compounds to determine the influence of the Fe substitution on the crystal structure and the magnetic properties of the hausmannite. Rietveld refinements of synthetic Fe-rich hausmannite neutron powder diffraction patterns at 295, 60, and 10 K indicate some significant and interesting changes of magnetic properties and crystal structure of hausmannite, which are directly linked to an increasing amount of iron substituting for manganese. The unit-cell parameters of $\text{Mn}_{3-x}\text{Fe}_x\text{O}_4$, in particular, illustrate decreasing Jahn-Teller distortion with increasing Fe content, whereas the Curie temperature was found to increase significantly with increasing Fe content. Nevertheless, this study indicates that the presence of Fe-rich hausmannite causes the unusual high-temperature ferrimagnetic behavior in the Kalahari manganese field.

INTRODUCTION

Hausmannite, ideally Mn_3O_4 , is a magnetically hard material with a tetragonal distorted spinel structure. It commonly accompanies other Mn-oxide minerals in metamorphosed or hydrothermal manganese ores (Frenzel 1980). However, macroscopic, euhedral crystals of hausmannite, typically in the pseudo-octahedral habit of a tetragonal bipyramid, are scarce and have only been described from a few localities, including Ilmenau, Thuringia (Germany) and the giant Kalahari manganese field, Northern Cape Province (South Africa). Recently, fine-grained and massive hausmannite-rich manganese ores have been described from Kalahari, which display an unusual, strongly ferrimagnetic behavior at room temperature (Gutzmer et al. 1995). These unusual magnetic properties were attributed by Gutzmer et al. (1995) to the presence of Fe-rich hausmannite, which contains up to 11.3 wt% of Fe_2O_3 . Mössbauer spectroscopy suggested that all iron in the magnetic hausmannite samples is trivalent (Gutzmer et al. 1995). Furthermore, the ferrimagnetic state of hausmannite is stabilized and enhanced by replacement of Mn^{3+} by Fe^{3+} , an effect that is also obvious in other spinels of the Mn_3O_4 - Fe_3O_4 group, although on a different scale. Curie temperatures increase in these Néel ordered spinels with increasing Fe content, e.g.,

from 413 K in Mn_2FeO_4 (synthetic ferrite) to 563 K in MnFe_2O_4 (jakobsite) and 858 K in Fe_3O_4 (magnetite). The purpose of this study is to test this tentative conclusion of Gutzmer et al. (1995).

PROPERTIES OF PURE HAUSMANNITE

Nuclear structure

The $[\text{Mn}^{2+}\text{Mn}_2^{3+}\text{O}_4]$ is a “normal” spinel compound, with divalent Mn^{2+} ions in the tetragonal site (Goodenough and Loeb 1955; Sinha et al. 1957; Satomi 1961; Boucher et al. 1971; Jensen and Nielsen 1974; Chardon and Vigneron 1986). A cubic high temperature phase appears above 1473 K (Frenzel 1980). Below this temperature, the compound $[\text{Mn}^{2+}\text{Mn}_2^{3+}\text{O}_4]$ has the tetragonal symmetry (space group no. 141, $I4_1/amd$) of a distorted spinel structure, with the O atom in position (16h), the Mn^{2+} ($3d^5$) ions in a (4a) tetrahedral site and the Mn^{3+} ($3d^4$) ions in a weakly distorted octahedral site (8d) (Satomi 1961). At room temperature, the lattice constants for the body-centered tetragonal unit cell are $a = b = 5.7691(4)$ Å and $c = 9.4605(7)$ Å (Satomi 1961). The oxygen position $y_o = 0.4723(3)$ and $z_o = 0.2592(2)$, is determined by the balance between the co-operative Jahn-Teller distortion around the Mn^{3+} site, stretching the spinel-lattice along [001], countered by the force of the tetrahedron preserving its regular form against the tetragonal deformation of the crystal (Satomi 1961; Sinha

* E-mail: Valery.Baron@studsvik.uu.se

et al. 1957). The chemical bonds in spinels are also known to influence the cation ordering, the lattice distortion, and the magnetic-exchange interactions (Goodenough and Loeb 1955). Four of the six O-metal bonds around the octahedrally co-ordinated Mn^{3+} cation are ionic, and only the two shortest bonds have a covalent character (Goodenough and Loeb 1955). In contrast, the O metal bonds around the tetrahedral sites are all semicovalent.

Magnetic properties

Chemically pure hausmannite is paramagnetic at room temperature (Frenzel 1980) and ferrimagnetic below a Curie temperature of 41.8(1) K (Boucher et al. 1971; Olés et al. 1976; Chardon 1986; Chardon and Vigneron 1986). The low Curie temperature is an obvious consequence of weak coupling between the Mn cations, which is easily disturbed by thermal excitation. The magnetic structure of hausmannite below the Curie point is fairly complex and has been studied by many authors (Kasper 1959; Boucher et al. 1971; Bonnet et al. 1974; Jensen and Nielsen 1974; Oles et al. 1976). Projected onto (001), the magnetic structure looks like a two-dimensional triangular Yafet-Kittel spin configuration (Boucher et al. 1971). This contrasts with the simple antiparallel Néel configuration present in other, more iron-rich members of the $\text{Mn}_3\text{O}_4\text{-Fe}_3\text{O}_4$ group of spinels (Gutzmer et al. 1995).

An anomaly in the magnetization curve of hausmannite at $T = 39$ K was attributed by Chardon (1986) and Chardon and Vigneron (1986) to a transition from a collinear incommensurate ($41.8 \text{ K} > T > 39 \text{ K}$) to a non-collinear commensurate ($T < 39 \text{ K}$) magnetic structure. The incommensurate part of the magnetic structure of hausmannite is sinusoidal (Jensen and Nielsen 1974; Chardon and Vigneron 1986), whereas below 33 K, the commensurate ferrimagnetic structure of hausmannite is described by eight magnetic sub-cells distributed on a chemical unit cell doubled in the **b** direction (Boucher et al. 1971; Jensen and Nielsen 1974). The magnetic unit cell has been previously determined by neutron diffraction on powder ($T = 4.2 \text{ K}$) and single crystal ($T = 4.7 \text{ K}$) by Boucher et al. (1971) and Jensen and Nielsen (1974). More recently, Chardon and Vigneron (1986) suggested a magnetic structure obtained by neutron powder diffraction at $T = 10 \text{ K}$. The three magnetic structures deviate somewhat from each other, but the components introduced for each of these models do not modify the selection rules for the magnetic Bragg peaks and do not introduce significant changes in the magnetic intensities.

Rietveld refinements in this study are based on the model proposed by Chardon and Vigneron (1986). In this model, the bonding electrons of the cations of different sublattices interact by direct exchange in the case of Mn^{3+} ions and/or by next neighbor cation-anion-cation superexchange in the case of $\text{Mn}^{3+}\text{-Mn}^{2+}$ and $\text{Mn}^{2+}\text{-Mn}^{2+}$ interactions. This superexchange coupling becomes stronger, the shorter the cation-oxygen bond length and the closer the cation-anion-cation bonding is to 180° (Anderson

1959). The exchange constants $J_{\text{Mn}^{2+}\text{Mn}^{2+}} = -4.9 \text{ K}$, $J_{\text{Mn}^{3+}\text{Mn}^{3+}} = -19.9 \text{ K}$, $J_{\text{Mn}^{2+}\text{Mn}^{3+}} = -6.8 \text{ K}$ are all antiferromagnetic. $\text{Mn}^{3+}\text{-Mn}^{3+}$ interaction is of predominant importance because of the relative short distance between two cations (Chardon 1986).

DATA COLLECTION AND REFINEMENT PROCEDURE

All neutron powder diffraction experiments were performed at the Studsvik R2 reactor in Sweden. During the course of this study, a new multidetector system was installed with 35 separate detectors and gadolinium-coated mylar collimators, replacing the previous system with only 10 detectors. The new configuration allows the choice between rapid scans of 6–8 h with a lower resolution of $\Delta d/d = 0.002$ and slower but more accurate scans taking 2 to 3 d with much higher resolution at higher scattering angles. The neutron flux at the sample position during this study was $2.10^6 \text{ n/cm}^2\cdot\text{s}$. A monochromator system with two Cu crystals (220) was used in parallel alignment ($\lambda = 1.470 \text{ \AA}$). The samples were contained in a vanadium cylinder during the data collection. Diffractograms were collected in the 2θ range $4\text{--}139.95^\circ$ with the new system and between 4.2 and 128.04° with the previous multidetector. The contributions from the detectors were statistically analyzed and added. Absorption effects were corrected in the Rietveld refinements by using experimental determined values of μR .

The data were analyzed using the Rietveld method (Rietveld 1969) implemented in the FULLPROF computer program (Rodriguez-Carjaval 1993). Refined parameters included one scale factor, one zero point, and five background coefficients B_m of a polynomial expression $y_i = \sum B_m(2\theta_i/90 - 1)^m$, with $0 \leq m \leq 5$. Two cell parameters a and c , three half-width parameters and a peak asymmetry correction for angles below 45° in 2θ were also refined. The peak shape was described by a pseudo-Voigt function with a Lorentzian contribution to the Gaussian form. Atomic co-ordinates and isotropic thermal parameters were adjusted to give the best agreement between the calculated and observed profiles. The site occupancies of Fe and Mn were refined for the data set collected in the paramagnetic phase at 295 K. The values obtained were introduced as constants into the refinement at 10 K.

In the nuclear part the neutron scattering lengths used for Fe, Mn, and O were respectively 9.45, -3.73 , and 5.803 fm. The magnetic form factors used in the magnetic refinements are those from the FULLPROF program (Rodriguez-Carjaval 1993).

RESULTS

Natural hausmannite, non-magnetic at room temperature

Neutron powder diffraction experiments at 295 and 10 K were performed on four natural hausmannite separates that were previously described by Gutzmer et al. (1995). Two of them are non-magnetic at room temperature, whereas the two others are concentrates of the magnetic

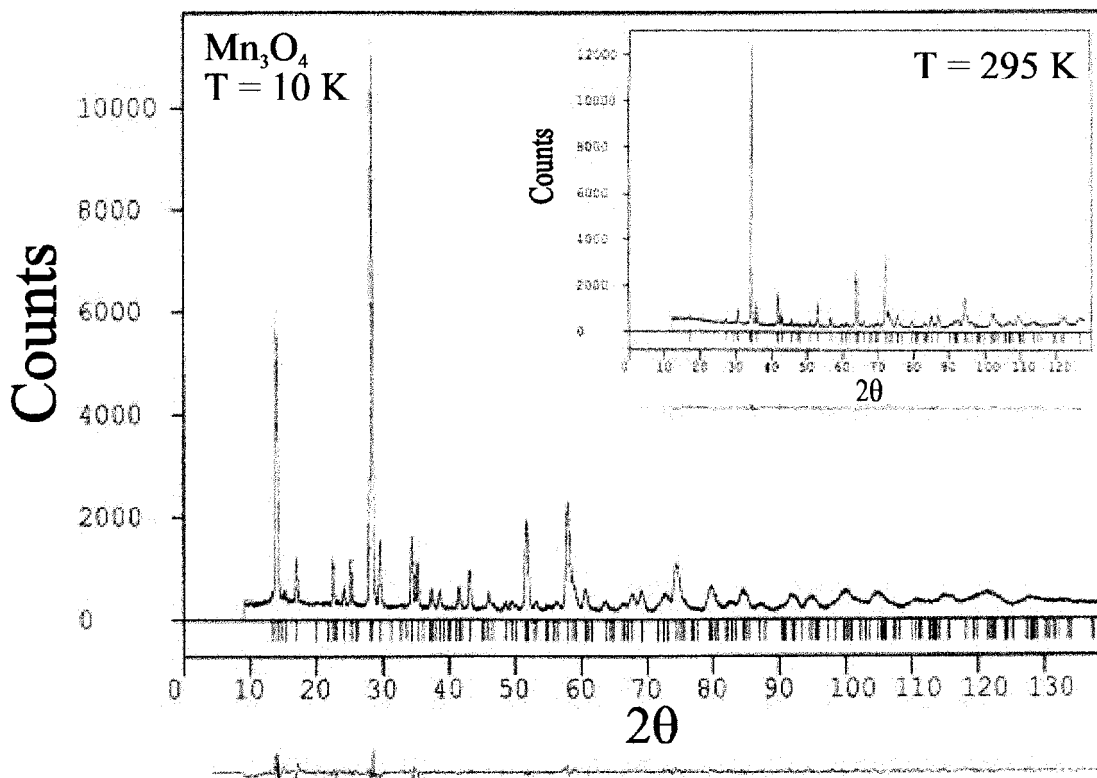


FIGURE 1. Neutron powder diffraction of Mn_3O_4 at 295 and 10 K.

fraction of fine crystalline and dense hausmannite ores that display strong ferrimagnetic behavior at room temperature (Gutzmer et al. 1995). Rietveld refinement of one of the two non-magnetic samples show it to be indeed chemically pure hausmannite devoid of measurable substitution of Fe for Mn (Fig. 1). The crystallographic and magnetic information retrieved from this sample (Table 1) are in good agreement with the results obtained by Chardon and Vigneron (1986) and form the basis for the study of natural and synthetic Fe-bearing hausmannite samples.

The second non-magnetic natural sample was found to be Fe-bearing hausmannite, $\text{Mn}^{2+}(\text{Mn}_{0.969}^{3+}\text{Fe}_{0.031}^{3+})_2\text{O}_4$, with about 2.5 at% Fe^{3+} substituting for Mn^{3+} (Fig. 2, Table

2). This Fe-bearing hausmannite sample is still magnetically ordered at 60 K, well above the Curie temperature of chemically pure hausmannite.

Natural Fe-rich hausmannite separates, magnetic at room temperature

Five phases [Fe-rich hausmannite, $\text{Mn}^{2+}(\text{Mn},\text{Fe})_2\text{O}_4$ (5.6% Fe in Mn sites); chemically pure hausmannite, $\text{Mn}^{2+}\text{Mn}_2\text{O}_4$; Mn-rich hematite, $(\text{Fe},\text{Mn})_2\text{O}_3$ (9.3% Mn in Fe sites); chemically pure hematite, Fe_2O_3 ; and small amounts of andradite, $\text{Ca}_3\text{Fe}_2\text{Si}_3\text{O}_{12}$] were identified in both concentrates of magnetic hausmannite ores. Only the andradite, present in minute amounts of <1 vol%, was excluded from the refinement procedure. Attempts were

TABLE 1. Nuclear and magnetic Rietveld refinement of $\text{Mn}^{2+}(\text{Mn}^{3+})_2\text{O}_4$ at $T = 10$ K

| | x | y | z | B | M_y | M_z | M |
|----------------------|-------|-----------|------------|-----------|----------|----------|---------|
| Mn^{2+} | 0.000 | 0.750 | 0.125 | 0.20(9) | 4.2(1) | — | 4.2(1) |
| Mn^{3+} (A) | 0.000 | 0.125 | 0.625 | 0.20(6) | -1.51(8) | -3.37(7) | 3.69(8) |
| Mn^{3+} (A) | 0.000 | 0.375 | 0.625 | 0.20(6) | -1.51(8) | 3.37(7) | 3.69(8) |
| Mn^{3+} (B) | 0.250 | 0.000 | 0.375 | 0.20(6) | -1.3(1) | -1.49(7) | 1.96(8) |
| Mn^{3+} (B) | 0.250 | 0.500 | 0.375 | 0.20(6) | -1.3(1) | 1.49(7) | 1.96(8) |
| O1 | 0.000 | 0.4729(3) | 0.2590(2) | 0.32(4) | — | — | — |
| | | a | b | c | | | |
| Nuclear structure | | 5.7574(4) | 5.7574(4) | 9.4239(9) | | | |
| Magnetic structure | | 5.7574(4) | 11.5147(8) | 9.4239(9) | | | |

Note: Space group is $I4_1/amd$, $\chi^2 = 2.18$, $R_p = 0.053$, $R_{wp} = 0.071$, $R_{exp} = 0.048$, $R_{mag} = 0.068$, and $R_{Bragg} = 0.021$.

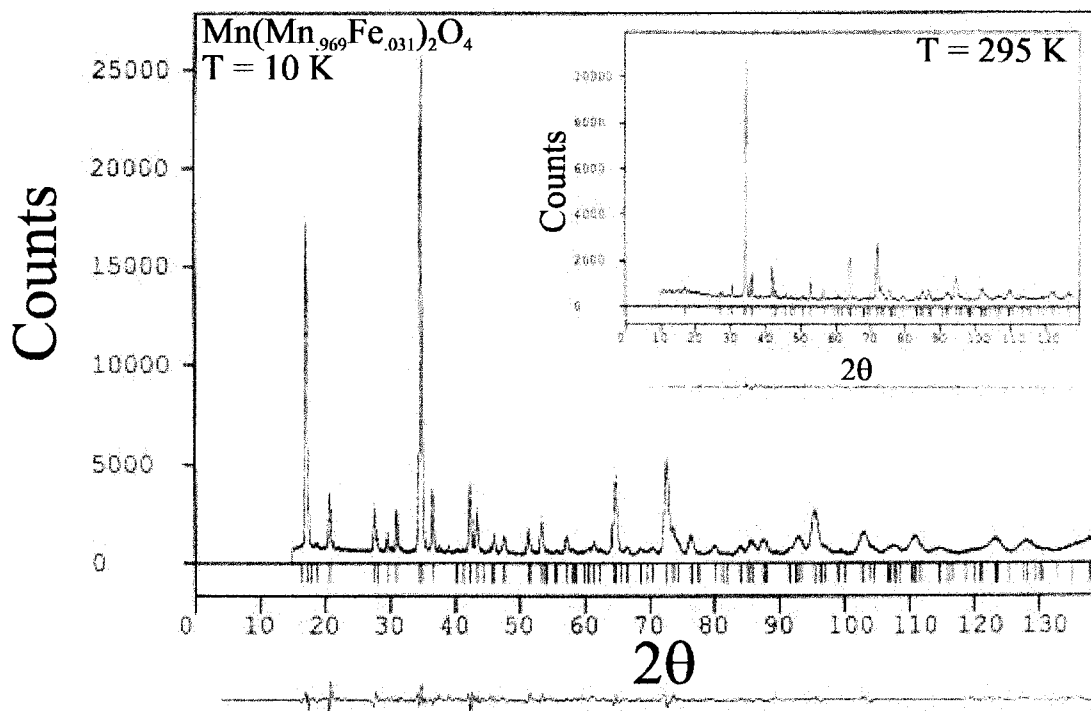


FIGURE 2. Neutron powder diffraction of $\text{Mn}(\text{Mn}_{0.969}\text{Fe}_{0.031})_2\text{O}_4$ at 295 and 10 K.

made to refine the crystallographic and the magnetic structures of all phases. However, the magnetic hausmannite separates were too impure to allow a reliable Rietveld refinement.

The most obvious crystallographic differences between Fe-rich hausmannite and chemically pure hausmannite are the unit-cell dimensions, which shrink along the a axis and expand somewhat along the c axis with increasing Fe content. More important is that the magnetic Bragg peak of hausmannite, a distinct expression of magnetic-ordering below the Curie temperature, is not observed at room temperature in the magnetic hausmannite separates. This observed lack of magnetic-ordering samples indicates that Fe-rich hausmannite is not the source of the macroscopically observed ferrimagnetism at room temperature.

Synthetic Fe-rich hausmannite

Fe-rich hausmannite was synthesized following the procedure described by Chardon (1984). Pure hausmannite samples were obtained, with Fe contents exceeding those of the natural samples. The two synthetic samples $\text{Mn}_{0.963}^{2+}\text{Fe}_{0.037}^{2+}(\text{Mn}_{0.901}^{3+}\text{Fe}_{0.099}^{3+})\text{O}_4$ and $\text{Mn}_{0.943}^{2+}\text{Fe}_{0.057}^{2+}(\text{Mn}_{0.880}^{3+}\text{Fe}_{0.120}^{3+})\text{O}_4$ have 7.8 and 9.9 at% Fe^{3+} contents, respectively. Neutron powder diffractometry and Rietveld refinements were at room temperature and 10 K. Results are displayed in Figure 3 and listed in Table 3 for the second sample.

DISCUSSION

Results of Rietveld refinement on all Fe-bearing natural and synthetic hausmannite samples suggest that iron is preferentially incorporated into the 8d octahedral site of the hausmannite lattice, substituting for Mn^{3+} . Mössbauer

TABLE 2. Nuclear and magnetic Rietveld refinement of $\text{Mn}^{2+}(\text{Mn}_{0.969}^{3+}\text{Fe}_{0.031}^{3+})_2\text{O}_4$ at $T = 10$ K

| | x | y | z | B | M_x | M_y | M_z | M |
|---------------------|-------|-----------|------------|-----------|---------|---------|---------|--------|
| (Fe,Mn) $^{2+}$ | 0.000 | 0.750 | 0.125 | 0.3(1) | — | -4.3(1) | — | 4.3(1) |
| (Fe,Mn) $^{3+}$ (A) | 0.000 | 0.125 | 0.625 | 0.00(9) | -2.2(1) | 1.6(1) | -4.0(1) | 4.8(1) |
| (Fe,Mn) $^{3+}$ (A) | 0.000 | 0.375 | 0.625 | 0.00(9) | 2.2(1) | 1.6(1) | 4.0(1) | 4.8(1) |
| (Fe,Mn) $^{3+}$ (B) | 0.250 | 0.000 | 0.375 | 0.00(9) | — | 1.5(1) | -0.8(2) | 1.8(1) |
| (Fe,Mn) $^{3+}$ (B) | 0.250 | 0.500 | 0.375 | 0.00(9) | — | 1.5(1) | 0.8(2) | 1.8(1) |
| O1 | 0.000 | 0.4736(3) | 0.2595(2) | 0.19(5) | — | — | — | — |
| | | a | b | c | | | | |
| Nuclear structure | | 5.7510(3) | 5.7510(3) | 9.3744(8) | | | | |
| Magnetic structure | | 5.7510(3) | 11.5020(6) | 9.3744(8) | | | | |

Note: Space group is $I4_1/amd$, $\chi^2 = 6.57$, $R_p = 0.058$, $R_{wp} = 0.080$, $R_{exp} = 0.031$, $R_{mag} = 0.048$, and $R_{Bragg} = 0.033$.

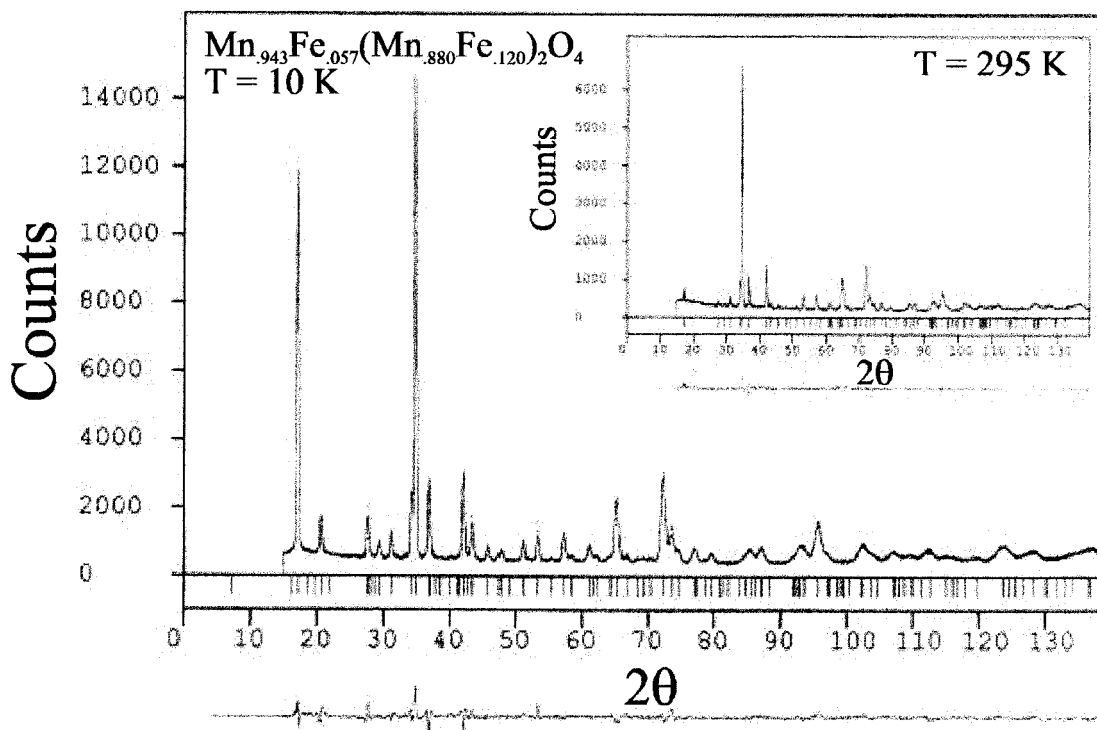


FIGURE 3. Neutron powder diffraction of $\text{Mn}_{0.943}\text{Fe}_{0.057}(\text{Mn}_{0.880}\text{Fe}_{0.120})_2\text{O}_4$ at 295 and 10 K.

spectroscopy, conducted on synthetic and natural Fe-bearing hausmannite samples, confirmed the presence of Fe^{3+} only. This result is corroborated by the tetragonal lattice distortion decreasing with increasing Fe^{3+} substitution (Buhl 1969), which is due to a co-operative Jahn-Teller effect around the octahedrally co-ordinated anisotropic Mn^{3+} ions. The observed change of the unit-cell parameters may indicate a distinct change of the crystal structure upon iron substitution. Figure 4 illustrates how the unit-cell parameters of hausmannite approach those of more Fe-rich ferrites, Mn_2FeO_4 , MnFe_2O_4 (jakobsite), and Fe_3O_4 (magnetite). Magnetite has undistorted spinel-type structure and Néel magnetic ordering is stable to temperatures well above room temperature ($T_C = 858$ K) (Gutzmer et al. 1995; Buhl 1969). Thus distinct changes of the magnetic structure are expected as well as a possible sta-

bilization of magnetic ordering to higher temperatures as a result of the incorporation of Fe into the hausmannite lattice. T_C measurements and previous data are reported Figure 4.

Lattice distortion and cation distribution also can be explained on the basis of the bond-forming properties of the Fe and Mn cations and their relative affinity for particular crystallographic sites (Sinha et al. 1957). Mn^{3+} - Fe^{3+} coupling can enforce spin coupling and may stabilize the ferrimagnetic state at higher temperature, especially if the distances between the cations are short and allow superexchange between Mn^{2+} and Fe^{3+} through the O^{2-} ions. The results indicate that the shortest bonds, between two Mn^{3+} ions, give rise to a direct exchange interaction, if the well-oriented orbitals are occupied. All longer bonds, between metallic ions, give rise to an indirect ex-

TABLE 3. Nuclear and magnetic Rietveld refinement of $\text{Mn}_{0.943}^{2+}\text{Fe}_{0.057}^{2+}(\text{Mn}_{0.880}^{3+}\text{Fe}_{0.120}^{3+})_2\text{O}_4$ at $T = 10$ K

| | <i>x</i> | <i>y</i> | <i>z</i> | <i>B</i> | <i>M_x</i> | <i>M_y</i> | <i>M_z</i> | <i>M</i> |
|---------------------------|----------|-----------|------------|----------|----------------------|----------------------|----------------------|----------|
| (Fe,Mn) ²⁺ | 0.000 | 0.750 | 0.125 | 0.0(1) | — | -4.5(1) | — | 4.5(1) |
| (Fe,Mn) ³⁺ (A) | 0.000 | 0.125 | 0.625 | 0.0(1) | -0.9(2) | 1.9(1) | -3.2(1) | 3.8(1) |
| (Fe,Mn) ³⁺ (A) | 0.000 | 0.375 | 0.625 | 0.0(1) | 0.9(2) | 1.9(1) | 3.2(1) | 3.8(1) |
| (Fe,Mn) ³⁺ (B) | 0.250 | 0.000 | 0.375 | 0.0(1) | — | 1.8(1) | -0.6(2) | 1.9(1) |
| (Fe,Mn) ³⁺ (B) | 0.250 | 0.500 | 0.375 | 0.0(1) | — | 1.8(1) | 0.6(2) | 1.9(1) |
| O1 | 0.000 | 0.4735(3) | 0.2596(2) | 0.12(6) | — | — | — | — |
| | | <i>a</i> | <i>b</i> | <i>c</i> | | | | |
| Nuclear structure | | 5.7779(4) | 5.7779(4) | 9.268(1) | | | | |
| Magnetic structure | | 5.7779(4) | 11.5557(9) | 9.268(1) | | | | |

Note: Space group is $I4_1/amd$, $\chi^2 = 3.58$, $R_p = 0.051$, $R_{wp} = 0.068$, $R_{exp} = 0.036$, $R_{mag} = 0.071$, and $R_{Bragg} = 0.050$.

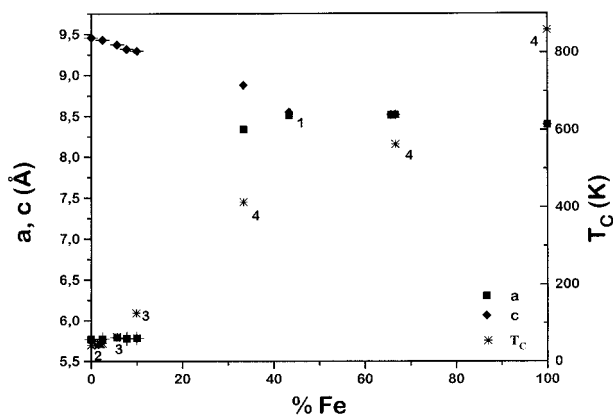


FIGURE 4. Variation of the unit-cell parameters and T_c as a function of the Fe content in $\text{Fe}_x\text{Mn}_{3-x}\text{O}_4$ (1 = Evans et al. 1988; 2 = Chardon 1986; 3 = H. Mazaki and S. Tochiohara, personal communication; 4 = Gutzmer et al. 1995).

change interaction (superexchange). Because hausmannite is usually paramagnetic at room temperature, and because we observe the substitution of Mn^{3+} by Fe^{3+} in the octahedral site, high-temperature ferrimagnetism could thus be explained by magnetic ordering of the octahedral sites alone. In this respect, Mn^{2+} and Fe^{3+} have identical electron configurations and therefore similar magnetic properties, so the substitution of one for the other should not result in any prominent change of the magnetic properties of hausmannite.

Pure hausmannite

The spontaneous magnetization of natural pure hausmannite at temperatures below T_c was determined to $1.4(2) \mu_B/\text{molecule}$ for a powder sample (Wickham and Croft 1958), in contrast to $1.87(2) \mu_B/\text{mol}$ inferred from single-crystal structure refinement of Dwight and Menyuk (1960). This well-known effect is readily explained by the reduction of the apparent magnetic moment by anisotropy effects in polycrystalline samples (Dwight and Menyuk 1960). The obtained values above are far less than the $3.0 \mu_B/\text{molecule}$ that would be expected, if a simple antiparallel Néel model of electron spin orientation was applied to magnetically ordered hausmannite (Dwight and Menyuk 1960). However, this effect is not unique to hausmannite because many other materials with spinel structure exhibit smaller spontaneous magnetization than necessitated by Néel ordering. In those cases the Yafet-Kittel theory of canted spins, or even more complex models of spin orientation, are applied to explain reduced magnetic moments (Dwight and Menyuk 1960).

The present Rietveld refinement of chemically pure hausmannite is in excellent agreement with existing models (Chardon 1984). At 10 K, the magnetic structure is three-dimensionally ordered and can be described by a doubling of the chemical unit cell along **b**. The 8 Mn^{2+} ions present on tetrahedral sites are ferromagnetically aligned parallel to [010], whereas the moments of the 16

Mn^{3+} ions on octahedral sites form a more complicated ordered configuration. All Mn^{2+} ions have a magnetic moment of $4.2(1) \mu_B$ along [010]. The resulting moment for Mn^{3+} ions is orientated antiparallel to the direction of the magnetic moment of the Mn^{2+} cations. The magnetic resultant for the octahedral site A of $3.69(8) \mu_B$ is distinctly greater than the resultant of the magnetic moment for the octahedral site B of $1.96(8) \mu_B$. It is obvious that the experimentally obtained individual magnetic moments are distinctly smaller than their theoretical Néel moment ($5 \mu_B$). In the octahedral site A, the absolute values obtained for M_y and M_z are $1.51(8) \mu_B$ and $3.37(7) \mu_B$. For site B, M_y and M_z were found to be $1.3(1) \mu_B$ and $1.49(7) \mu_B$, respectively.

For the $\text{Mn}^{2+}\text{-O}^{2-}$ bond a length of $2.044(2) \text{ \AA}$ was obtained, corresponding to a semicovalent character of the bond, intermediate between a calculated ionic bond length of 2.2 \AA and a calculated covalent bond length of 1.9 \AA . The bonds to the two apical O anions in the distorted octahedral site around the Mn^{3+} cation are $1.932(1) \text{ \AA}$, corresponding to a covalent bond (80% covalent and 20% ionic bond), whereas the bonds to the four remaining O atoms are ionic in character and $2.284(2) \text{ \AA}$. The shortest cation-cation distance between two Mn^{3+} ions is 2.885 \AA , permitting direct exchange interaction, if the well-orientated orbitals are occupied. All other cation-cation distances are longer than 3.123 \AA and will thus only permit indirect exchange interaction.

Fe-rich hausmannite

Natural Fe-bearing hausmannite with 2.5% Fe substitution is non-magnetic at room temperature, but remains magnetically ordered to at least 60 K. At $T = 10 \text{ K}$, the magnetic order is three-dimensional and similar to that of chemically pure hausmannite. Magnetic moments of the 8 Mn^{2+} ions are aligned parallel to [010], oriented antiparallel to the 16 Mn^{3+} moments (Fig. 5). All Mn^{2+} ions have a magnetic moment of $4.3(1) \mu_B$ along [010]. The difference between the resultant magnetic moments of the two octahedral sites A [$4.8(1) \mu_B$] and B [$1.8(1) \mu_B$] is much larger than for the chemically pure hausmannite. The M_x site B contribution is small and insignificant to the final magnetic model, but a significant M_x component of $2.2(1) \mu_B$ was established for the octahedral site A. Moments M_y and M_z for site A are $1.6(1) \mu_B$ and $4.0(1) \mu_B$, respectively, but only $1.5(1) \mu_B$ and $0.8(2) \mu_B$ for site B. The substitution of minor amounts of Mn^{3+} by Fe^{3+} in the octahedral site appears to increase the individual magnetic moment of these sites and stabilizes the magnetic ordering to slightly higher temperatures (Fig. 4), but decreases the spontaneous magnetization of the hausmannite by about 15%, from $1.4(2) \mu_B/\text{molecule}$ to $1.2(1) \mu_B/\text{molecule}$.

No evidence for magnetic moment ordering was found in the two synthetic Fe-rich hausmannite samples at $T = 295 \text{ K}$. The results observed for the two synthetic samples, with 7.8 and 9.9 at% Fe^{3+} (samples no. 1 and 2) repeat the observed absence of magnetic ordering in nat-

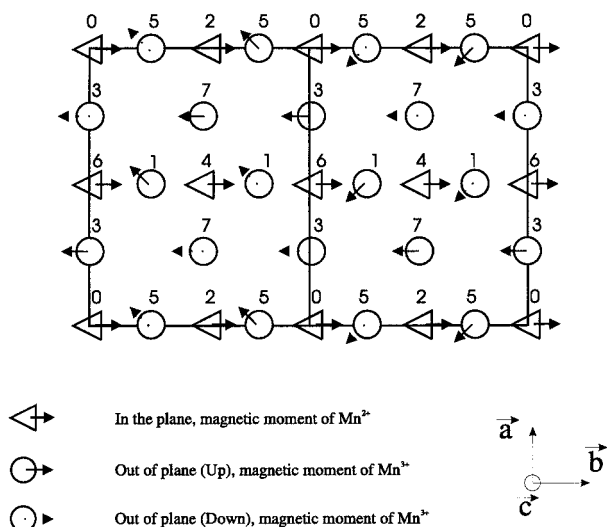


FIGURE 5. Magnetic structure of Fe-rich hausmannite phase at $T = 10$ K. The magnetic unit cell is described as twice the chemical unit cell. The numbers give the elevation $z/8$ for the different magnetic ions.

ural Fe-rich hausmannite at room temperature. The three-dimensional magnetic ordering in Fe-rich hausmannite at 10 K is similar to that described for chemically pure hausmannite. The unit cell of the magnetic structure corresponds to a doubling of the chemical unit cell along **b**. The magnetic moments of the 8 Mn^{2+} ions that occupy the tetrahedral sites in the unit cell are also aligned parallel to [010], with individual magnetic moments of 4.5 (1) μ_B for both samples. The magnetic moments of the 16 octahedrally co-ordinated Mn^{3+} ions, on the other hand, form a complex configuration; the resultant of the magnetic moment for the octahedral co-ordinated Mn^{3+} ions being oriented antiparallel to the Mn^{2+} moments.

The resultant moment for the octahedral site A is 3.9(1) μ_B for sample no. 1 and 3.8(1) μ_B for sample no. 2, it is always greater than the resultant of the magnetic moment for the octahedral site B, which is 1.9(1) μ_B for both samples. The M_x component for the octahedral site B is still too small to be of any significance in the final magnetic model. For site A, however, the M_x component is significant and appears to decrease with increasing Fe content from 1.0(1) μ_B for sample no. 1 to 0.9(1) μ_B for sample no. 2. The components M_y and M_z for site A are equal to 1.7(1) μ_B and 3.3(1) μ_B for sample no. 1 and 1.9(1) μ_B and 3.2(1) μ_B for sample no. 2. M_y and M_z for site B, on the other hand, are 1.8(1) μ_B and 0.7(2) μ_B for sample no. 1 and 1.8(1) μ_B and 0.6(2) μ_B for sample no. 2. The decrease of the spontaneous magnetization, from 1.0(1) μ_B /molecule for sample no. 1 to 0.8(1) μ_B /molecule for sample no. 2, appears to be the result of the increase of the magnetic moments at the octahedral sites A and B; which correspond to a decrease of 22.5% from sample no. 1 to sample no. 2 and 43% relative to the spontaneous magnetization of chemically pure hausmannite.

CONCLUSIONS

Substitution of Mn^{3+} on octahedral sites by Fe^{3+} results in minor, but measurable changes in the unit-cell constants, indicating a decrease of Jahn-Teller distortion with increasing Fe^{3+} concentrations. The magnetic structure changes little at temperatures below the Curie point. The complex, three-dimensional spin configuration remains virtually unaffected even at highest iron concentrations. Changes include a slight but distinct increase of the Curie point and a strong decrease of the spontaneous magnetization with increasing iron substitution. Both observations argue convincingly against the suggestion that Fe-rich hausmannite is the source for high-temperature ferrimagnetism in hausmannite-rich ores from the Kalahari manganese field. Minor amounts of Mn-bearing hematite in the hausmannite-rich ores may constitute the source for the unusual magnetic properties described by Gutzmer et al. (1995). Experimental studies are in progress to test the hypothesis that the substitution of Fe by Mn in hematite results in a strong increase of spontaneous magnetization and a decrease of the Curie temperature from 948 K for pure hematite to 750 K for Mn-bearing hematite.

ACKNOWLEDGMENTS

The authors are grateful to H. Mazaki and S. Tochihara for the T_C measurements they performed at the National Defence Academy, Yokosuka, Japan. We also thank Françoise Bourée (Laboratoire Léon Brillouin-C.E.N. Saclay) for discussions and help in providing information on the hausmannite.

REFERENCES CITED

- Anderson, P.W. (1959) New approach to the theory of superexchange interactions. *Physical Review*, 115, 2–13.
- Boucher, B., Buhl, R., and Perrin, M. (1971) Propriétés et structure magnétique de Mn_3O_4 . *Journal of Physics and Chemistry of Solids*, 32, 2429–2437.
- Buhl, R. (1969) Manganites spinelles purs d'éléments de transitions préparations et structures cristallographiques. *Journal of Physics and Chemistry of Solids*, 30, 805–812.
- Chardon, B. (1986) Etude de la structure magnétique des oxydes mixtes Mn_3O_4 - $ZnMn_2O_4$. Thèse de l'université de Paris VI.
- Chardon, B. and Vigneron, F. (1986) Mn_3O_4 commensurate and incommensurate magnetic structures. *Journal of Magnetism and Magnetic Materials*, 58, 128–134.
- Dwight, K. and Menyuk, N. (1960) Magnetic properties of Mn_3O_4 and the canted spin problem. *Physical Review*, 119, 5, 1470–1479.
- Evans, B.J., Dunham, W.R., Porter, C., Abernathy, S.M., and Bluncson, C. (1988) Crystal/chemical structures and magnetic properties of naturally occurring $Mn_{1-x}Fe_xO_4$. *Journal of Applied Physics*, 63, 4133–4135.
- Frenzel, G. (1980) The manganese ore minerals. In I.M. Varentsov and G. Grassely, Eds., *The geology and geochemistry of manganese*, p. 25. Schweizerbarth, Stuttgart.
- Goodenough, J.B. and Loeb, A.L. (1955) Theory of ionic ordering, crystal distortion, and magnetic exchange due to covalent forces in spinels. *Physical Review*, 98, 391–408.
- Gutzmer, J., Beukes, N.J., Kleyenstüber, A.S.E., and Burger, A.M. (1995) Magnetic hausmannite from hydrothermally altered manganese ore in the paleoproterozoic kalahari manganese deposit, Transvaal Supergroup, South Africa. *Mineralogical Magazine*, 59, 703–716.
- Jensen, G.B. and Nielsen, O.V. (1974) The magnetic structure of Mn_3O_4 (hausmannite) between 4.7 K and the Néel point, 41 K. *Journal of Physical Chemistry: Solid State Physics*, 7, 409–424.
- Kasper, J.S. (1959) Magnetic structure of hausmannite, Mn_3O_4 . *Bulletin of the American Physics Society*, 4, 178.

- Olés, A., Kajzar, F., Kucab, M., and Sikora, W. (1976) Magnetic structures determined by neutron diffraction. Warzow, 727.
- Rietveld, H.M. (1969) A profile refinement method for nuclear and magnetic structures. *Journal of Applied Crystallography*, 2, 65.
- Rodriguez-Carjaval, J. (1993) ILL, Internal report. FULLPROF computer program.
- Satomi, K. (1961) Oxygen positional parameters of tetragonal Mn_3O_4 . *Journal of the Physical Society of Japan*, 16, 258–266.
- Sinha, A.P.B., Sanjana, N.R., and Biswas, A.B. (1957) On the structure of some manganites. *Acta Crystallographica*, 10, 439–440.
- Wickham, D.G. and Croft, W.J. (1958) Crystallographic and magnetic contribution properties of spinels containing trivalent JA-1044 manganese. *Journal of Physics and Chemistry of Solids*, 7, 351–360.

MANUSCRIPT RECEIVED JULY 14, 1997

MANUSCRIPT ACCEPTED FEBRUARY 15, 1998

PAPER HANDLED BY LEE A. GROAT